Moroccan Journal of Chemistry
ISSN: 2351-812X
http://revues.imist.ma/?journal=morjchem&page=login
Alaoui & al. / Mor. J. Chem. 9 N°3 (2021) 454-463

Structural study, thermal and physical properties of K_2O-CaO-P_2O_5 phosphate glasses

Y. Alaoui [(a)], M. El Moudane [(a)], A. Er-rafai [(a)], M. Khachani [(a)], A. Ghanimi [(a)], A. Sabbar [(b)], M. Tabyaoui [(a)], A. Guenbour [(a)], A. Bellaouchou [(a)]

[(a)] Laboratory of Materials, Nanotechnology and Environment, Mohammed V University in Rabat, Faculty of Sciences, Av. Ibn Batouta Av., PB. 1014, Rabat, Morocco

[(b)] Laboratory of Spectroscopy Molecular Modeling Nanomaterial Materials Water and Environment, of Mohammed V University in Rabat, Faculty of Sciences, Ibn Battouta Av., PB. 1014, Rabat, Morocco

** Corresponding author:*
m.elmoudane@gmail.com
Received 28 Aug 2020,
Revised 11 Oct 2021,
Accepted 25 Oct 2021.

Abstract

Glasses of $50P_2O_5$-xCaO-(50-x)K_2O (x= 0, 10, 20, 30, and 40 mol %) compositions were synthesized using the melt-quench procedure. The amorphous character of the prepared material was confirmed by X-ray diffraction (XRD) and Differential Scanning Calorimetry (DSC). Fourier Transform Infra-Red (FT-IR) and Raman spectroscopy are also carried out to determine the structural network evolution of the glassy materials with the composition. Besides, the physical properties of the glassy phosphate system were examined such as density and molar volume. The results showed that the increase of CaO content in phosphate glasses diminish the molar volume and raise the density and transition temperature. FTIR and Raman spectroscopy analysis demonstrate the formation of P-O-Ca bonds that substitute P-O-K bonds and the depolymerization of the phosphate chains. The formation of P-O-Ca bonds is in accordance with variations of glass transition temperature, (Tg), molar volume (Vm), and density (ρ). The former bonds are the origin of the partial glass-forming ability of Ca^{2+}. Also, an analysis of the surface morphology features was conducted using a Scanning Electron Microscopy (SEM) technique.

Keywords: *Phosphate glasses, Glass transition temperature, Density, Molar volume, DSC, Infrared and Raman spectroscopy, SEM.*

1. Introduction

Compared to silicate and borate glasses, phosphate based-glasses have shown in the last decades numerous advantages such as very bass melting temperature, reduced crystallization ability, important electrical conductivity, lower transition temperature, greater UV transmission, etc. [1-3]. Despite that, their applications in many fields are still limited, due principally to their hygroscopic nature and the low chemical durability [4]. However, multiple investigations have been implemented to enhance the properties of glasses; therefore, it was shown that introducing some alkali metal oxides and alkaline earth metals oxides such as K_2O and CaO is an excellent solution to improve physical properties and chemical durability, and to intensify their moisture-resistance [4]. CaO was found to be a great glass stabilizer that could form a stable matrix with P_2O_5 and material solubility tailor [5-9]. While, K_2O was extensively used as a glass fluxes to diminish the working temperature, although it also plays an essential part in setting the thermal expansion. Glasses carrying phosphorus and calcium in their composition form an interesting field of research based on the development of useful biomaterials for bone regeneration [10]. Numerous in vitro and in vivo studies revealed good biocompatibility of glasses when used in hard and soft tissue healing [11]. These glasses have valuable features explored as reinforcement phases for composite biomaterials and drug delivery systems. Their potential use was as fibers in tissue engineering, principally for any tissue with a medium to high anisotropy, such as muscles, and as dental restoratives, etc. [12,13]. However, the compositional variation that can be used for the binary glassy system $CaO-P_2O_5$ is limited. This system is hard to process due to high thermal expansion coefficients and exhibits excessive dissolution rates. Therefore, in order to develop more practical system, it is required to improve the complexity and use of ternary systems. Ahmina et al. [14] have examined the role of manganese in $K_2O–MnO–P_2O_5$ ternary system phosphate which can be a valuable comparative data to the present study. They reported that the density and glass transition temperature augment with the substitution of MnO for K_2O. Further, Ahmed et al. [15, 16] have studied the sodium-calcium phosphate ternary glassy system P_2O_5-CaO-Na_2O. They found that this system was the center of biomedical domain because of its composition containing elements existing throughout the human body and also for its low dissolution rate described by the substitution of the monovalent sodium oxide (Na_2O) with the divalent calcium oxide (CaO). Recently, Marikani et al. [17] have synthetized and characterized the calcium phosphate $P_2O_5–CaO–Na_2O–K_2O$ glass system. The obtained results indicate that the glassy studied are bioactive materials. Generally, the functionality of glasses (processing, properties and applications) had considerably presented in Karmakar's book published in 2017 [18]. According to our survey, no data has been reported on the structural, thermal en physical properties of calcium phosphate glass system containing potassium oxide. This work aims at investigating the structural features of a new glass with various compositions $50P_2O_5$-xCaO-(50-x)K_2O (with x= 0, 10, 20, 30, and 40 mol %). The new developed glass composition is based on replacing potassium oxide (K_2O) by calcium oxide (CaO) while keeping the amount of phosphorus oxide (P_2O_5) as fixed. FTIR, Raman spectroscopies, and SEM coupled to EDS were used for the structural characterization of the studied system. Furthermore, thermal and physical properties i.e. glass transition temperature (T_g), density (ρ), and molar volume (V_m) were investigated and the results were correlated with the structural behavior.

2. Materials and methods

2.1. Phosphate glasses preparation

The calcium phosphate glasses samples of the system $50P_2O_5$-xCaO-(50-x)K_2O, with x= 0, 10, 20, 30, and 40 mol%, were elaborated using appropriate amounts of precursors, ammonium dihydrogen phosphate ($NH_4H_2PO_4$), calcium carbonate ($CaCO_3$,) and potassium carbonate (K_2CO_3). Firstly, the precursors were weighed, well mixed in a quartz mortar before be transmitted in a porcelain crucible to preheat at 120°C overnight. After that, the mixture was annealed at 400°C for four hours to eliminate byproducts (i.e., H_2O, NH_3, and CO_2). Then, the temperature was gradually

increased to the melting temperature, which is in the range of 800-900°C. Finally, vitreous specimens were obtained after quenching the melted product to the room temperature under air condition. From the first appearance, all the glassy samples have transparent aspect (Figure 1), except the composition with x equals 0 mol % which looks semi-transparent. All samples were well saved in desiccator to evade moisture attack.

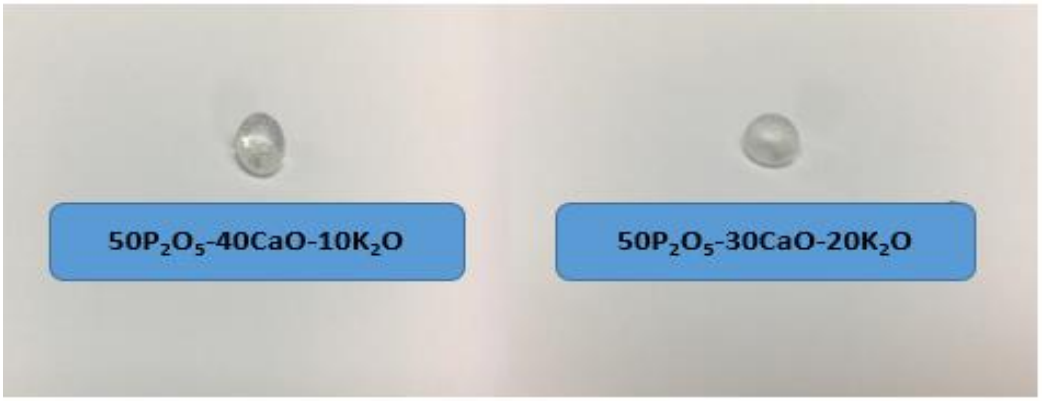

Figure 1. Photograph of two synthesized glassy sample.

2.2. Phosphate glasses characterization

2.2.1. X-ray diffraction

X-ray diffraction (XRD) analysis has been used many times to prove that the synthesized products are of amorphous structure. Spectral data were collected using a Siemens D5000 diffractometer with Cu_λ radiation (λ =1,5418Å) in the 2θ ranges of 10° to 60° with a scanning rate of 2° per minute at room temperature.

2.2.2. Density and molar volume

The measure of density for the synthesized glassy samples was performed at room temperature by the Archimedes technique using diethyl phthalate as the reference immersion liquid. The density was assessed by the relation:

$$\rho = W_a \rho_b / (W_a - W_b)$$

Where, W_a and W_b are the weight of the glass sample in air and in the buoyant solution, respectively. (W_a-W_b) is the buoyancy, and ρ_b is the buoyant density.

The molar volume V_m of each glass was evaluated from the density ρ and the molecular weight M according to:

$$V_m = \rho / M$$

2.2.3. Thermal study

Differential scanning calorimetry (DSC) analysis has been employed to identify the glass transition temperature (T_g). DSC results were achieved by utilizing the DSC-SETRAM type apparatus 121, under a heating rate of 10°C/min, with an estimated error of ±5°C.

2.2.4. Fourier transform infrared spectroscopy (FTIR)

Fourier transform infrared spectroscopy (FTIR) measurements were conducted to identify phosphate glasses phases. The data were collected using a spectrometer Jasco 4600 FT/IR type A with frequency ranging 4000-400 cm^{-1} and a resolution of 4 cm^{-1}.

2.2.5. Raman spectroscopy

Raman spectra were recorded at room temperature using a Raman micro-spectrometer Renishaw RM1000 connected to a red He-Ne laser (19 mW) with line of 632.8nm. The spectra were gathered from 200 cm^{-1} and 1400 cm^{-1}.

2.2.6. Scanning Electron Microscopy (SEM)

Scanning Electron Microscopy (SEM) was applied to investigate the microstructural morphology of glassy materials surface. The images were registered by utilizing Joel-JSM-IT-100 scanning electron microscope coupled to a micro-analyzer EDS.

3. Results and discussion

The glass composition, density (ρ), molar volume (V_m), and glass transition temperature (T_g) of the studied samples are ground in Table 1. The obtained results showed that ρ and T_g increase while augmenting CaO contents, whereas V_m diminishes progressively.

Table1. Glass composition (mol %), density **ρ** ($g.cm^{-3}$), molar volume $\mathbf{V_m}$ ($cm^3.mol^{-1}$) and glass transition temperature $\mathbf{T_g}$ (°C) of $50P_2O_5$-xCaO-(50-x)K_2O glasses

Glass no.	Batch composition			ρ	V_m	T_g
	K_2O	CaO	P_2O_5			
1	50	0	50	2.30 ± 0.01	52.34 ± 0.01	254 ± 5
2	40	10	50	2.43 ± 0.01	50.54 ± 0.01	300 ± 5
3	30	20	50	2.48 ± 0.01	47.98 ± 0.01	341 ± 5
4	20	30	50	2.49 ± 0.01	46.26 ± 0.01	386 ± 5
5	10	40	50	2.57 ± 0.01	43.17 ± 0.01	471 ± 5

3.1. X-Ray diffraction

The XRD diagrams of the five studied compositions, of $50P_2O_5$-xCaO-(50-x)K_2O glassy system (where x=0, 10, 20, 30 and 40 mol%), illustrate a broad boss between 20° and 40° (2 Theta) with absence of any sharp peaks confirming, therefore, the amorphous nature of these glassy phosphates (Figure 2).

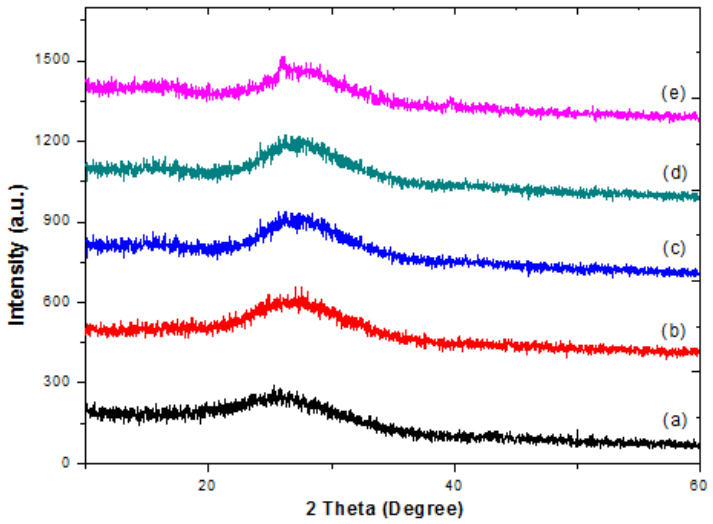

Figure 2. X-ray diffraction patterns for the five compositions studied of $50P_2O_5$-xCaO-(50-x)K_2O glasses, with: (a) x=0 mol%, (b) x=10 mol%, (c) x=20 mol%, (d) x=30 mol%, and (e) x=40 mol%

3.2. Density and molar volume

The density is an important tool used to explore the level of variations in the phosphate glasses structure. However, it is affected by the compactness of the glassy structure. The glass network density (ρ) and molar volume (V_m) depend on numerous factors, i.e., structure, coordination number, cross-link density and dimensionality of interstitial spaces [19]. The plots of ρ and V_m values are graphically presented in Figure 3**.** It is well shown that the ρ values augment with the gradual rise of the CaO contents from 2.30 g/cm^3 (for x=0 mol%) to 2.57 g/cm^3 (for x=40 mol%). This result could be imputed to the replacement of K_2O which has low-density (2.35 g/cm^3), by CaO that has high-density (3.34 g/cm^3). Likewise, this comportment may also be due to the differences in atomic mass of Ca^{2+} and K^+. On the other hand, V_m decreases continuously when substituting K_2O by CaO, from 52,34 cm^3/mol for x=0 mol% to 43,17cm^3/mol for x=40 mol%. This could be attributed to the fact that K^+ cations are bigger than Ca^{2+} cations, thereby, the cations exchange lead to the shortness in the chain length. Thus, the phosphate glasses network becomes compact and reticule with a closing in the structure [14].

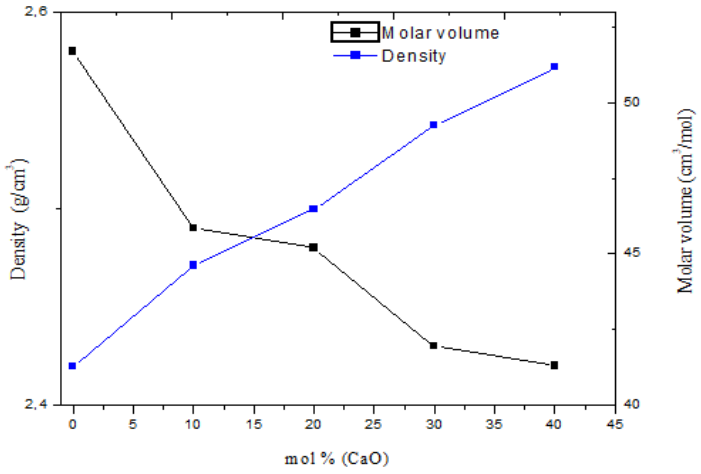

Figure 3. Density and molar volume as function of CaO content of $50P_2O_5$-xCaO-(50-x)K_2O glasses.

3.3 DSC study

Figure 4 represents an illustrative DSC curve of the synthesized glassy sample of the system $50P_2O_5$-xCaO-(50-x)K_2O with x= 20 mol %. DSC results show variations in Tg values, from 254°C for potassium phosphate to 471°C after introduction of 20 mol% of calcium oxide (CaO) (Figure 5). Thus, it can be concluded that the substitution of K_2O by CaO lead to a remarkable rise of T_g (217°C) and therefore a strong modification in the glass structure based on the development of new bonding. After introduction of CaO, P-Ca-O bonds are formed with a strong Ca-O covalent bond due to the electronegativity of Ca (1eV), which is larger than K (0.82 eV). The bond P-O-Ca formed has an important covalent character in accordance with the increase of T_g [14].

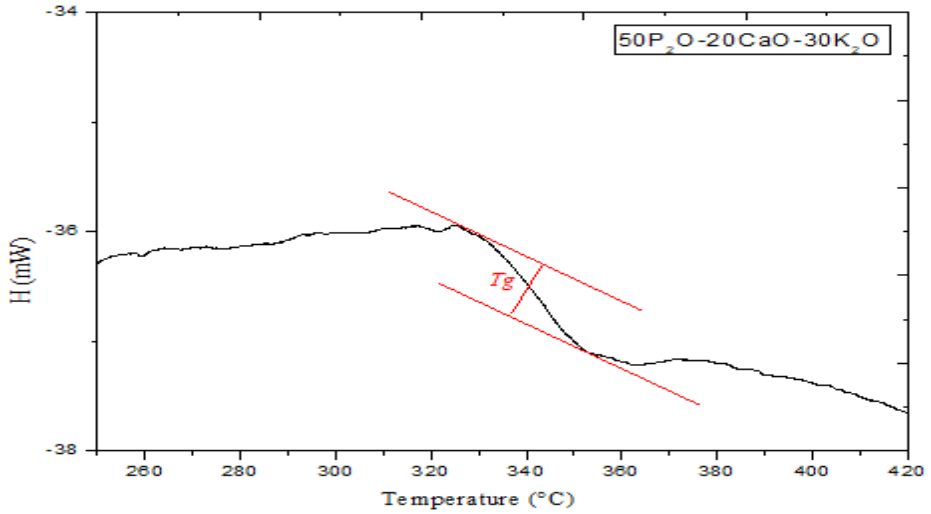

Figure 4. DSC curve of the synthesized glassy sample $50P_2O_5$-20CaO-30K_2O.

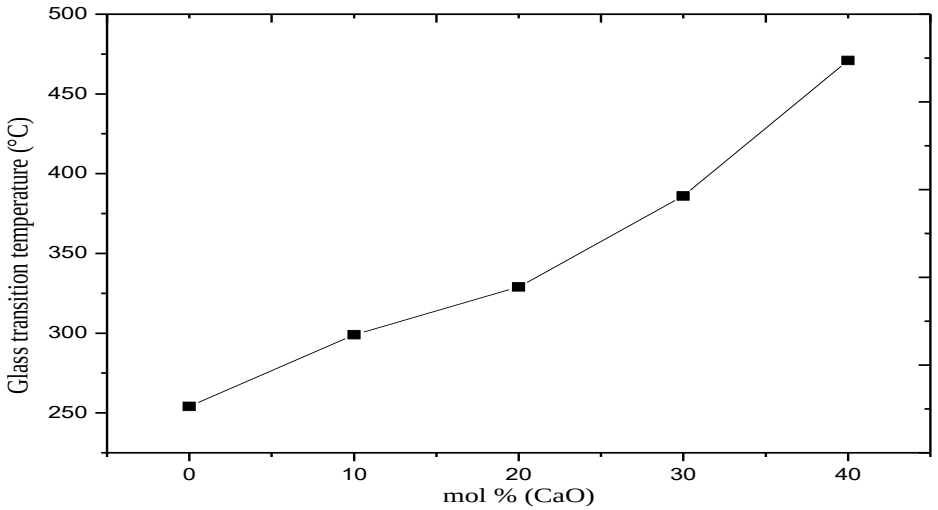

Figure 5. Glass transition temperature as a function of CaO content for $50P_2O_5$-xCaO-(50-x)K_2O glasses.

3.4 FTIR spectroscopy

The FT-IR spectra of the glass samples are shown in Figure 6. The diverse vibration bands were identified based on the literature [14, 20, 21]. The remarked bands at 1265 cm^{-1} are associated to the asymmetric stretching vibration $\nu_{as}(PO_2)$ of the bonds linking atoms, of oxygen non-bridged (ONB) with phosphorus [22-26]. While, the bands around 1180 cm^{-}

[1] are ascribed to the symmetric stretching vibration $\nu_s(PO_2)$ [27, 28]. The presence of bands near 1095 cm^{-1} are assigned to the asymmetric stretching-vibration $\nu_{as}(PO_3)$. However, those nearby 1000 and 990 cm^{-1} are attributed to chain end groups [29]. The lines associated to asymmetric and symmetric stretching vibrations of P-O-P bridges are observed, respectively, at around 880 cm^{-1} and at 800-760 cm^{-1} [24-30]. The bands located at 530 cm^{-1} corresponds to the deformational modes of P-O^- (PO_4^{3-}) groups [31]. The inclusion of CaO into K_2O-P_2O_5 causes the disappearance of $\nu_{as}(PO_3)$ and the reduction in the intensity of $\nu_s(PO_3)$. This phenomenon is due to the fact that PO_3 is pretended as a phosphate chain ending group. Besides, the apparition of P-O-Ca bonds in the glass network, when CaO substitute K_2O, provokes the development of the ONB and the growth in the crosslinking. The depolymerization of P-O-P bonds in the analyzed glassy samples is mainly due to the rise of CaO content, causing a slight change in the spectra [14, 32]. Furthermore, the existence of pyrophosphate groups could be explained by the presence of two specific bands at 880 and 760cm^{-1} related respectively to the symmetric and asymmetric vibrations of P-O-P Bridge [33]**.**

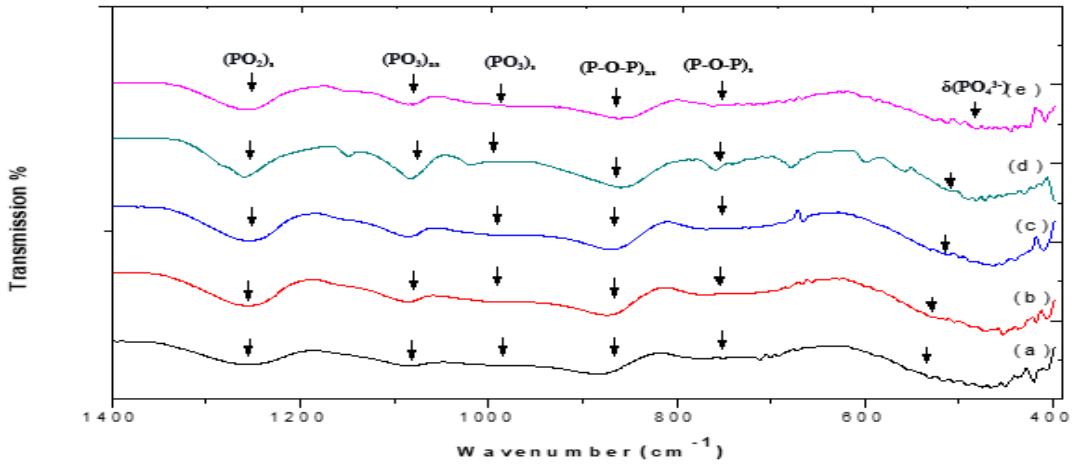

Figure 6. FTIR spectra of $50P_2O_5$-xCaO-(50-x)K_2O glasses with: (a) x=0mol%, (b) x=10mol%, (c) x=20mol%, (d) x=30mol% , and (e) x=40mol%.

3.5 Raman spectroscopy

Figure 7 illustrates the Raman spectra of $50P_2O_5$-xCaO-(50-x)K_2O glasses (where x= 0, 10, 20, 30 and 40 mol%). The spectra reveal six peaks at 1175, 1098, 990, 780, 680 and 555 cm^{-1}. The band located at 1175 cm^{-1} is attributed to the symmetric vibration $\nu_s(PO_2)$ of the oxygen atoms non-bridged (ONB) which are linked to the phosphorus atoms (O-P-O) in metaphosphate chains (Q^2) [34-36]**.** While, the bands observed at 1098 cm^{-1} and 990 cm^{-1} are characteristic of the asymmetric $\nu_{as}(PO_3)$ and the symmetric vibrations $\nu_s(PO_3)$ of ONB in Q^1 tetrahedral [14]**.** The bands sited at 780 and 680 cm^{-1} are associated with the asymmetric and symmetric stretching modes of oxygen bridged and related to phosphorus atoms (P-O-P), where two tetrahedral are connected in the phosphate chains [28-30]**.** However, the band situated at 555 cm^{-1} is correlated to the deformation modes of P-O^- (PO_4^{3-}) groups [35]**.**

The addition of CaO conducts to progressive changes in the spectra, particularly for the band located at 1175 cm^{-1} , corresponding to the phosphate glass sample with x=40mol%. Yet, the intensity of the band at 680 cm^{-1} diminishes gradually. These variations can be associated with disturbance of the bridges P-O-P the depolymerization of phosphate chains driving, therefore, to the formation of phosphate dimers Q^1 when the O/P ratio augments [35, 36]**.** On the other hand, a new peak appeared at about 910 cm^{-1} for x=30mol%, which can be ascribed to the asymmetric stretching vibration of the ONB in PO_4 tetrahedron in pyrophosphate units [36]**,** where its intensity rises with CaO contents.

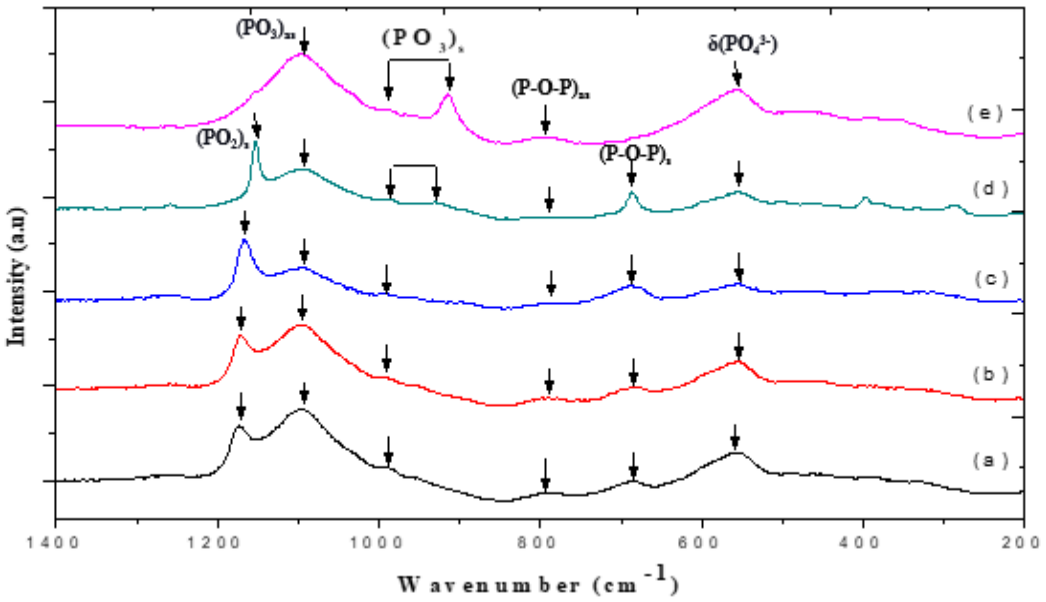

Figure 7. Raman spectra of $50P_2O_5$-xCaO-(50-x)K_2O glasses with: (a) x=0 mol %, (b) x=10 mol %, (c) x=20 mol %, (d) x=30 mol %, and (e) x=40 mol %.

3.6 Scanning Electron Microscopy (SEM)

SEM image of $50P_2O_5$-30CaO-20K_2O glassy phosphate is displayed in Figure 8**.** It can be observed the presence of a porous surface. The EDS data collected from two places on the surface of, $50P_2O_5$-30CaO-20K_2O illustrate the main components existing in the network of the studied glassy phosphate.

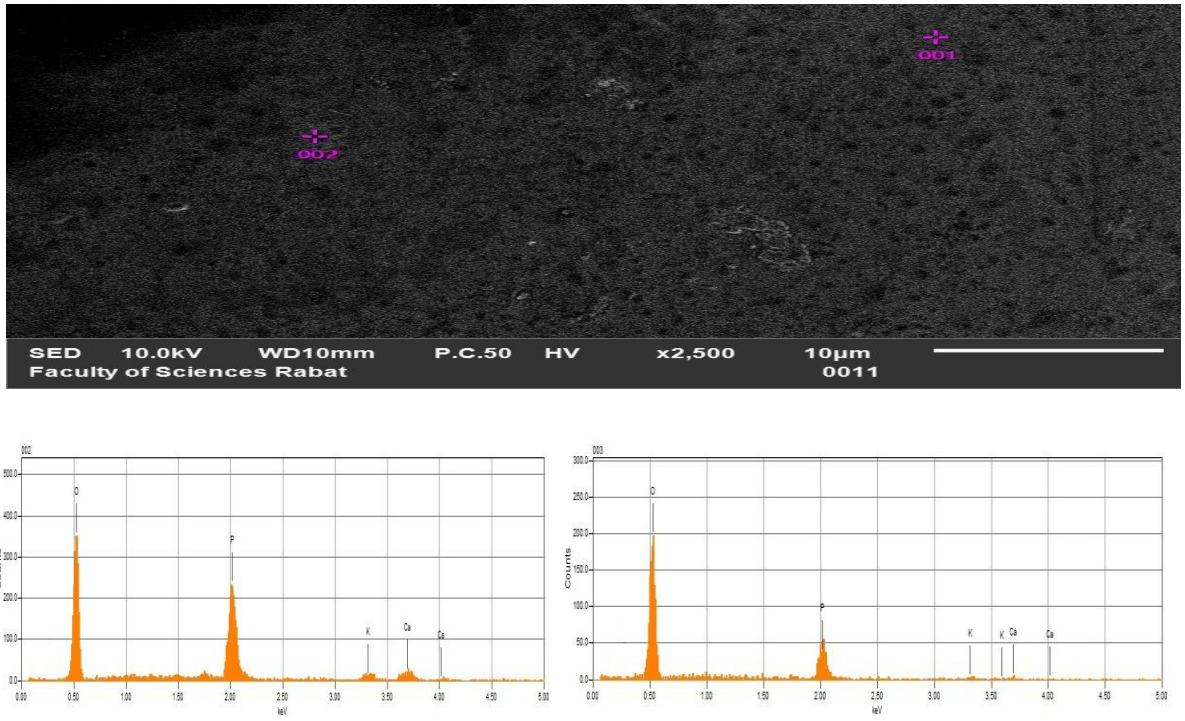

Figure 8. SEM image and EDS of $50P_2O_5$-30CaO-20K_2O glassy sample

4. Conclusion

A series of potassium-phosphate glasses with varying CaO concentrations is successfully prepared using the melt quench technique. The X-ray diffraction results have proved that there is no crystalline peak to be identified, which confirms the amorphous phase of the prepared samples. DSC measurements revealed that glass transition temperature increases with CaO content. The density presents a growing trend from 2.30g/cm^3 to 2.57g/cm^3 and the molar volume drops progressively from 52.34 cm^3/mol to 43.17cm^3/mol, because of the increase in CaO content. DSC measurements revealed that T_g progresses with the addition of CaO content. FTIR and Raman spectroscopic analysis were carried out to clarify the structural evolution of the five synthesized glassy samples, when calcium oxide displaces potassium oxide, phosphate chains are depolymerized by the association of CaO into P-O-Ca bonds. The SEM proved that the synthesized glassy samples revealed homogeneity of the surface with the absence of any pores.

References

[1] M.R. Reidmeyer, D.E. Day, J. Mater. Res., 6 (1991) 1757–1762.

[2] M.R. Reidmeyer, D.E. Day, J. Non-Cryst. Solids, 181 (1995) 201–214.

[3] Y.M. Moustafa, A. El-Adawy, Phys. Status Solidi A, 179 (2000) 83–93.

[4] K. A. Matori, M. I. Sayyed, H. A. A. Sidek, M. H. M. Zaid, V. P. Singh, J. Non-Cryst. Solids, 457 (2017) 97-103.

[5] P. Y. Shih, Mater. Chem. Phys., 80 (2003) 299-304.

[6] B. Lakshmana Rao, Y. N. Ch. Ravi Babu, P. Syam Prasad, S. V. G. V. A. Prasad, Spectrosc. Lett., 48 (2015) 90-95.

[7] Y. B. Peng, D.E. Day, Glass Technol., 32 (1991) 166.

[8] L. Koudelka, P. Mošner, M. Zeyer, C. Jäger, J. Non-Cryst. Solids, 72 (2003) 326–327.

[9] D. Carta, D. M. Pickup, J. C. Knowles, I. Ahmed, M. E. Smith, R. J. Newport, J. Non-Crystal. Solids, 353 (2007) 1759-1765.

[10] A. Matamoros-Veloza, K. M. Zakir Hossain, B. E. Scammell, I. Ahmed, R. Hall, N. Kapur, J. Mech. Behav. Biomed. Mater., 102 (2020) 103489.

[11] S. Mokhtari, K. D. Skelly, E. A. Krull, A. Coughlan, N. P. Mellott, Y. Gong, R. Borges, A. W. Wren, J. Mater. Sci., 52 (2017) 8886-8903.

[12] M. Canillas, P. Pena, H. Antonio, A. R. Miguel, Bol. Soc. Esp. Ceram. Vidrio, 56 (2017) 91-112.

[13] J. C. Knowles, E.A. Abou Neel, V. Salih, J. Mater. Chem., 13 (2003) 2395-2401.

[14] W. Ahmina, M. El Moudane, M. Zriouil, M. Taibi, Phase Transitions, 89 (2016) 1–11.

[15] I. Ahmed, M. Lewis, I. Olsen, J.C. Knowles, Biomaterials, 25 (2004) 491–499.

[16] I. Ahmed, M. Lewis, I. Olsen, J.C. Knowles, Biomaterials, 25 (2004) 501–507.

[17] A. Marikani, A. Maheswaran, M. Premanathan, L. Amalraj, J. Non-Cryst. Solids, 354 (2008) 3929–3934.

[18] B. Karmakar, Functional Glasses and Glass-Ceramics: Processing, Properties and Applications. Butterworth-Heinemann (2017).

[19] F.A. Khalifa, Z.A. El-Hadi, F.A. Moustaffa, J. Pure Appl. Phys., 27 (1989) 279-281.

[20] W. Ahmina, M. El Moudane, M. Zriouil, M. Taibi, J. Mater. Environ. Sci., 7 (2016) 694-699.

[21] A.M. Aliyu, R. Hussin, N. E. Ahmad, A. Yamusa, Optik, 172 (2018) 1162-1171.

[22] M. Abid, M. Belfaquir, M. Hafid, M. Taibi, J. Mater. Environ. Sci., 9 (2018) 2788-2797.

[23] M. El Hezzat, M. Et-tabirou, L. Montagne, Phys. Chem. Glasses, 44 (2003) 345-348.

[24] H. S. Liu, T. S. Chin, S.W. Yung, Mater. Chem. Phys., 50 (1997) 1-10.

[25] E. Laengle, N. Hackerman, J. Electrochem. Soc., 118 (1971) 1273–1278.

[26] K.C. Pillai, R. Narayan, Corros. Sci., 23 (1983) 151–166.

[27] R. K. Brow, D.R. Tallant, S.T. Myers, C. C. Phifer, J. Non- Cryst Solids, 191 (1995) 45-55.
[28] L. Montagne, G. Palavit, G. Mairesse, Phys. Chem. Glasses, 37 (1996) 206-211.
[29] D. E.C. Corbridge, J. Appl. Chem., 6 (1956) 456-465.
[30] M. El Hezzat, M. Et-tabirou, L. Montagne, E. Bekaert, G. Palavit, A. Mazzah, P. Dhamelincourt, Mater. Lett, 58 (2003) 60-66.
[31] A. Chahinne, M. Et-tabirou, M. Elbenaaissi, M. Haddad, J.L. Pascal, Mater. Chem. Phys., 84 (2004) 341-347.
[32] F. Bartholomew Roger, J. Non-Cryst. Solids, 7 (1972) 221-235.
[33] M.A. Salim, G.D. Khattak, M. Sakhawat Hussain, J. Non-Cryst. Solids, 185 (1995) 101–108.
[34] N. Kerkouri, M. Haddad, M. Et-tabirou, A. Chahine, L. Laânab, Physica B, 406 (2011) 3142–3148.
[35] R.O. Omrani, S. Krimi, J. J. Videau, I. Khattech, A. El Jazouli, M. Jema, J. Non-Cryst. Solids, 389 (2014) 66–71.
[36] N. Zotov, H. Schlenz, B. Brendebach, H. Modrowa, J. Hormesa, F. Reinauerc, R. Glaumc, A. Kirfel, C. Paulmannd, Z. Naturforsch., A: Phys. Sci., 58 (2003) 419–428.